SLAC-PUB-5021
July 1989
(A)

# REQUIREMENTS AND LIMITATIONS ON BEAM QUALITY IN SYNCHROTRON RADIATION SOURCES*

**M. Cornacchia**
Stanford Linear Accelerator Center Stanford University, Stanford, CA 94309 USA

ABSTRACT

The requirements and limitations of the third generation of synchrotron radiation facilities are reviewed. These machines are designed to emit radiation of very high intensity, extreme brightness, very short pulses, and laserlike coherence. These performance goals put severe requirements on the quality of the electron or positron beams. Phenomena affecting the injection process and the beam lifetime are discussed.. Gas desorption by synchrotron radiation, collective effects (coupled bunch oscillations) and ion trapping (for an electron beam) play an important role. Low emittance lattices are more sensitive to quadrupole movements and at the same time, in order not to lose the benefits of high brilliance, require tighter tolerances on the allowed movement of the photon beam source.

## 1. INTRODUCTION

Third-generation synchrotron radiation sources are characterized by an increased emphasis on the ***qualify*** of the photon beam, expressed in terms of its ***spectral brightness.*** A high spectral brightness requires high-photon beam intensity, narrow spectral distribution and ease of focusing onto a small spot. A high photon brightness implies ***a low emittance*** of the electron beam:

Electron beam emittance $\approx$ minimum diffraction limited emittance.

or, for 0.5-1.0 keV photons,

$$\text{Emittance} \approx 10^{-8} \text{ mrad.}$$

The study and understanding of low-emittance lattices has made great progress over the last few years: optics like the Chasman-Green, FODO, enlarged Cbasman-Green, and Triple-Bend Achromat, have been studied in great depth [I]. All these lattices are characterized by the fact that, in order to achieve a low emittance, the dispersion and horizontal p-function at the location of the bending magnets must be small. This condition requires a strong focusing electron optics. A strong focusing optics has the disadvantage of requiring strong cbromaticity correction sextupoles and increased sensitivity to quadrupole misalignment and movement. Strong chromaticity correction sextupoles reduce the maximum amplitude of stable betatron oscillations that can be sustained in the vacuum chamber, and this, as we shall see, negatively impacts the electron beam lifetime. An increased sensitivity to quadrupole positioning errors leads to movement of the source. The benefits of high brilliance are compromised if the photon source moves. The challenge of the new generation of light sources is that the same optics characteristics that produce a high-brightness photon beam also make it difficult to obtain a long beam lifetime and stable operating conditions.

* Work supported by Department of Energy contract DE-AC03-76SF00515.

***Presented at the CERN/Daresbury Course on Synchrotron Radiation and Free Electron Lasers, Chester, England, April 6-13, 1989.***

Another important feature of third-generation light sources is the presence of a large number of long insertion devices. Wigglers and undulators constitute a strong perturbation to the lattice, and their linear and nonlinear effects must be taken into account in the design and operation of the storage rings.

With the increased power of synchrotron radiation sources as research tools, the operational requirements have also become more demanding in terms of:

- Flexibility (variable wavelength, adjustable optics, etc.).
- Reliability.
- Long, uninterrupted periods of photon delivery to the users.

For many experiments, very short, intense light pulses are required, with variable time intervals.

In the course of this lecture, we discuss some beam dynamics effects that are believed to constitute important limitations to the performance of a synchrotron radiation source. We divide the presentation into three parts:

- ***Acceptance-related effects:*** These limitations arise due to the finite acceptance of the storage ring (physical aperture, dynamic aperture and momentum acceptance). Examples: injection and accumulation efficiency, gas and intrabeam scattering lifetimes.
- ***Nonacceptance-related instabilities:*** Coupled-bunch oscillations, single-bunch instabilities, ion trapping.
- ***Photon beam movement.***

The effect of insertion devices on the beam dynamics is an important aspect of the new generation of light sources: it is discussed in other parts of these proceedings [1].

We will refer to the particles as "electrons," bearing in mind that, with the exceptionbf ion trapping, the beam instabilities discussed in this paper apply equally well to positrons. Section 3.3 contains a brief discussion on the choice between the two types of particle.

## 2. ACCEPTANCE-RELATED EFFECTS

We assume that the reader is familiar with the concepts of dynamic aperture and momentum acceptance. The beam size in a synchrotron radiation source is very small, as is required by the condition of high brilliance.-Typically, for a 1.5–2.0 GeV machine like the Advanced Light Source [2]:

- Horizontal beam size (standard deviation): 300 $\mu$m.
- The required horizontal half-aperture is much larger, of the order of 2-3 cm.

The relative momentum spread in the beam is of the order of 0.001 (standard deviation), whereas the required momentum acceptance can be as large as 0.03 (RF bucket half-height).

The physical aperture and the momentum acceptance are designed to be much larger than the transverse beam size and momentum spread. As a matter of fact, aperture and momentum spread are determined, not by the size of the core of the beam, but rather by the following conditions:

- *The* injection ***process*** requires aperture to accommodate the initial oscillations of the injected beam. A good injection efficiency is required to achieve the design beam intensity in a reasonably short time (of the order of a few minutes).

- ***Elastic*** scattering of electrons against the ***residual*** gas requires aperture in order not to lose the scattered particles, a necessary requirement for a long lifetime.
- ***Scattering*** between particles in the same beam ***(Touschek effect)*** and inelastic scattering against the residual gas requires both momentum acceptance and physical aperture in order not to lose the scattered particles. This is, again, a necessary condition for a long lifetime.

Another important source of aperture requirement is the well-known process of quantum excitation, both in betatron and momentum space [3]. In the energy regime under consideration (a few GeV) and for high-brilliance machines, the aperture requirements due to quantum excitation are easily satisfied if the above conditions (injection, Touscbek and gas-scattering effects) are satisfied also.

Finally, the physical aperture of the vacuum chamber must not be too small in order not to reduce the vacuum conductivity of the pipe. At the required pressure of $1 \times 10^{-9}$, vacuum considerations, as we shall see, play a major role in the design of the storage ring.

After a brief discussion on the dynamic aperture, we will review the aperture-limiting effects listed above.

## 2.1 The dynamic aperture and momentum acceptance

It is beyond the scope of this review to treat in detail the complex aspects of the nonlinear motion in an accelerator [4]. It is sufficient here to comment qualitatively on the implications of strong focusing on the dynamic aperture.

If the betatron motion were purely linear, the available aperture would be determined by the physical aperture (vacuum chamber). Sextupole magnets, nonlinear elements, are required to avoid the "bead-tail" instability [5] and to prevent resonance crossing and loss of particles subject to inelastic collisions. Because of the sextupole field, the equations of motion are now not linear:

$$\begin{aligned} \frac{d^2x}{ds^2} + K_x(s)\, x &= S(s)\,(x^2 - y^2) \\ \frac{d^2y}{ds^2} + K_y(s)\, y &= -2S(s)\, xy \end{aligned} \tag{1}$$

where $s$ is the distance along the synchronous orbit, $x$ and y are the horizontal and vertical oscillation amplitudes, $K_x(s)$ and $K_y(s)$ are the focusing terms, and S(s) is the sextupole strength.

The perturbing effect of a strong sextupolar perturbation distorts the phase-space motion of a particle. Typically, close to the dynamic aperture limit, the phase space is distorted, as shown in Fig. 1. It is possible to reduce the phase-space distortions by introducing more sextupole families to cancel some of the resonances driven by the cbromaticity sextupoles [6].

There is a rich literature describing the behavior of a particle in phase space. We recognize the following stages of nonlinear behavior as a function of the starting coordinates of a particle in phase space:

- At small amplitudes, the motion is quasilinear; the tunes are close to their linear values.
- As the oscillation amplitudes of the injected particles increase, the phase-space motion becomes more distorted and the tunes change quadratically with the betatron amplitudes.

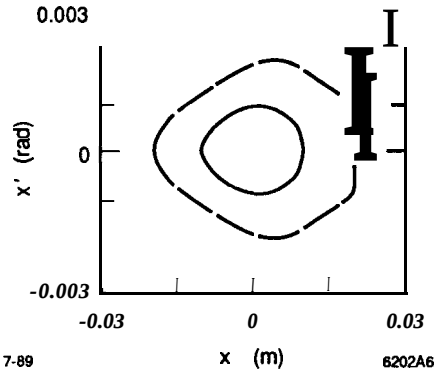


*Figure 1: Horizontal phase space distorted by the presence* of sextupole *magnets.*

- At even larger amplitudes, "island chains" with chaotic layers are formed. The tunes vary more rapidly than quadratically with amplitude.

- Close to the stability limit, the islands are now large enough to overlap. The motion is "chaotic." The initial particle amplitudes for which this phenomenon occurs are commonly called the dynamic ***aperture.***

We are interested here in relating the dynamic aperture to the conditions of high-photon brilliance. A low-beam emittance is achieved by strong focusing (small p-function and dispersion in the bending magnets). Strong focusing leads to high chromaticities, strong sextupoles, and reduced dynamic aperture. Similarly, the motion of an off-momentum particle is affected by the sextupole field. The momentum acceptance of a strong focusing electron optics is usually smaller than the one-obtained with more relaxed lattices.

The dynamic aperture is sensitive to the degree of symmetry of an accelerator, high periodicity being usually associated with a larger dynamic aperture. A high-lattice periodicity implies that systematic betatron resonances are widely spaced, and, thus, farther from the resonance overlapping criterion normally associated with the dynamic aperture limit [7]. Unfortunately, even in a machine designed with high periodicity, the regular lattice pattern is broken by magnetic imperfections, orbit errors and the presence of different types of insertion devices in different straight sections.

Figure 2 illustrates the fact that new generations of light sources (APS, Elettra, Advanced Light Source, Super ACO, PEP with a high-brilliance lattice) have a smaller dynamic aperture than those of older and more conservatively built machines (SPEAR, UV-NSLS, Aladdin) [8].

## 2.2 The injection process

In order to accumulate a high-electron intensity, several (of the order of 100 or more) beam pulses are required from the injector. The beam is injected off-axis from a bending magnet (the septum), designed in such a way that its field does not perturb the circulating beam. A typical injection process consists of the following steps [depicted in Figs. 3(a) and (b)].

- The stored beam is moved close to the septum as much as is allowed by the need not to lose any part of the particles in its tail. Normally, a distance from the septum equivalent to five beam-size standard deviations is considered acceptable.

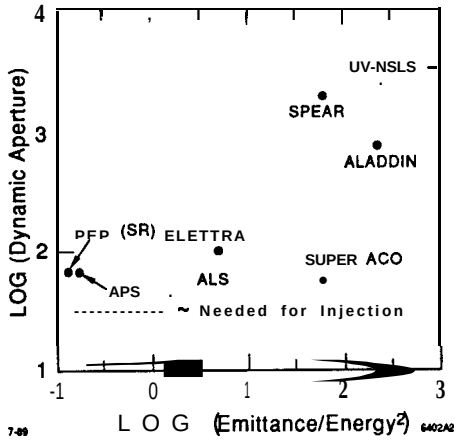


*Figure 2: Dynamic aperture of new generation (ALS, Elettra, Super ACO, PEP as a synchrotron radiation (SR) source,* i.e., *with a high brilliance optics, APS) and older machines (SPEAR, UV-NSLS, Aladdin). The decimal logarithm of the dynamic aperture* (in *mm mrad)* is *plotted against the decimal logarithm of the emittance (in $10^3$ mm mrad) divided by the square of the energy* in *GeV. The square energy* factor **normalizes** *the dependence of the emittance with energy. The broken line* is *meant to give an approximate* **idea** *of the acceptance needed for injection.*

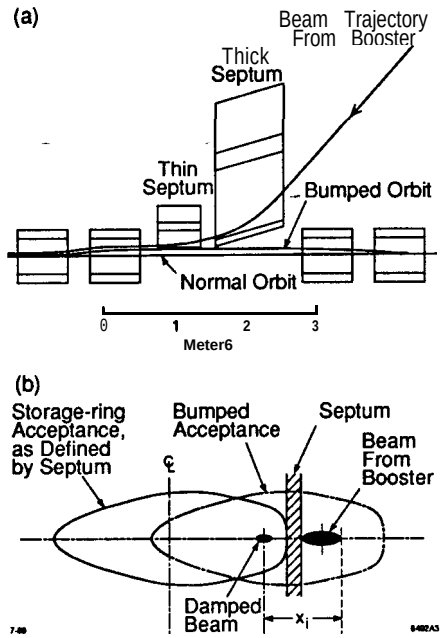


*Figure 3: (a) Anamorphic diagram of the storage ring injection process. Figure credit:* Fig. *3–8, ALS Conceptual Design Report, LBL Report Pub-5172 (b) Storage ring acceptance, bumped beam acceptance, and the injected beam* in *radial phase space, at the end of the septum magnet. The* **center** *lines shown are for the vacuum vessel.* **Figure** *credit: Fig. 3-9, ALS Conceptual* Design *Report, LBL Report Pub-5172*

- The orbit of the injected beam follows the septum boundary at a distance of the order of four times its rms size (since the aperture limitation only acts on the beam for a single crossing, the injected beam can be allowed to be closer to the septum than the circulating beam).
- The injected beam enters the storage ring. Since it is injected off-axis, it executes betatron oscillations.

At the septum location, the maximum amplitude of the oscillations, $X_i$, is given by

$$X_i = 8\sigma_I + t + 5\sigma_c$$

where $\sigma_I$ and $\sigma_c$ are the rms sizes of the injected and circulating beams, respectively. $X_i$ is of the order of 15-20 mm, depending on the beam emittance, lattice functions, septum thickness, and safety factors. The amplitude $X_i$ propagates around the ring following the modulation of the p-function, attaining its maximum value where the p-function is largest. It is good design practice to have a p-function at the septum as large as possible, in order to minimize the oscillation amplitude anywhere else in the ring.

Typically, a minimum dynamic aperture of the order of 15-20 mm is required by the injection process. Failuretoachieve this aperture makes it necessary to move the circulating and injected beam closer to the septum and, as a likely consequence, loss of particles during the injection process.

The conditions of efficient injection represent the strictest and most uncompromising requirement of the design, since it fundamentally affects the performance of the storage ring.

### 2.3 Gas scattering

The interactions of the circulating beam with the atoms of the residual gas can be of two types:

- ***Elastic.*** The electron receives an angular kick without experiencing a change in its energy. The scattering starts a betatron oscillation. The particle is lost if the amplitude of the oscillation exceeds the available aperture (dynamic-or physical, whichever is smaller).
- ***Inelastic.*** The electron energy changes at the point of- the interaction. The particle describes synchrotron oscillations and is lost if the amplitude of the oscillation exceeds the momentum acceptance of the machine. At the same time, betatron oscillations are also excited, if, at the location of the energy change, the value of the dispersion function and/or its derivative is nonzero. Because of the energy change, the particle finds itself displaced from the closed orbit appropriate to the new momentum and describes betatron oscillations around the new orbit.

In this context, only single scattering events need to be considered, since, for the vacuum pressures which are required for a long lifetime, the average time interval between consecutive interactions is much longer than the radiation damping times.

In what follows, we briefly describe the types of interactions that are possible, and the expressions for the associated lifetimes. We also give a brief introduction to the main cause of gas emission in synchrotron radiation sources, namely ***photodesorption.***

#### 2.3.1 Gas scattering lifetime

- ***Elastic*** scattering on nuclei.

The effect is an angular deflection. The cross section for the process is given by [9]:

$$\sigma_1 = \frac{4r_e^2 Z_i^2 \pi}{\gamma^2 \theta_0^2} \quad , \tag{2}$$

where $Z_i$ is the atomic number of gas species i, $r_e$ is the Lorentz radius of the electron, and $\theta_0$ is

the angle associated with betatron amplitudes greater than the available horizontal and vertical half-apertures $a, b$. The aperture restriction usually occurs in the vertical plane (undulator gap). In this case

$$\theta_0 = \frac{2b^2}{\beta_u \bar{\beta}} ,$$

where $\beta_u$ is the vertical p-function at undulator, and $\bar{\beta}$ is the average vertical p-function around the ring.

- ***bremsstrahlung on nuclei.***

$$\sigma_2 = \frac{4r_e^2 Z_i^2}{137} \frac{4}{3} \left[\ln\left(\frac{183}{Z_i^{1/3}}\right)\right]\left[\ln\left(\frac{1}{(\Delta P/P)_{lim}}\right) - \frac{5}{8}\right] , \tag{3}$$

where $(\Delta P/P)_{lim}$ is the maximum relative momentum deviation accepted by the storage ring.

This process has a very weak dependence on energy.

The above are the most important processes; elastic and inelastic scattering on electrons have much smaller cross sections.

For a given cross section, the ***lifetime*** is given by

$$\frac{1}{\tau} = -\frac{1}{N}\frac{dN}{dt} = \sigma_t \, cn$$
$$\sigma_t = \sigma_1 + \sigma_2 , \tag{4}$$

where n = 3.22 x $10^{22}$ P ($n$ in $m^{-3}$; P in Torr.) for a monatomic gas at 300° K, and c is the electron velocity.

Normally, one sets

$$\sum_i Z_i^2 P_i \approx P Z_{eq}^2 , \tag{5}$$

where $P$ is the total pressure, $Z_{eq}$ = 7-10 (typically, for nitrogen, Z = 7).

From Eqs. (2) and (3), one sees that elastic scattering becomes more important at low energy, and bremsstrahlung at high energy.

In third-generation light sources, the most important aperture limitation is given by the gap of the insertion devices, which could be as small as 1 cm. Figure 4 shows the lifetime due to gas scattering as a function of the total pressure in the SRRC synchrotron radiation source at 1.5 GeV [10].

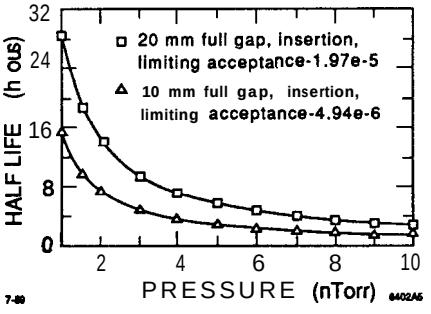


***Figure 4: Gas-scattering lifetime as a function of total gas pressure*** in ***the 1.3 Ge V Synchrotron Radiation Source currently under construction*** in ***Taipei, Taiwan, Republic of China.***

### 2.3.2 Photodesorption

Figure 4 indicates that a vacuum pressure of 1-2 nTorr is required in the SRRC storage ring. This low pressure is a common requirement of the new generation of light sources. To maintain a vacuum level of 1 nTorr in the presence of synchrotron radiation is a difficult technological problem. Photons emitted by synchrotron radiation produce photoelectrons when they strike the vacuum chamber walls. The photoelectrons desorb gas. An important empirical quantity is the gas desorption coefficient, defined as the number of molecules produced per incident photon: $N_{mol} = \eta N_{ph}$. Typically, this number is of the order of $10^{-5}$ to $10^{-7}$, depending on the conditions of the chamber wall. Several experiments have been carried out at various laboratories (CERN, Daresbury, KEK) to measure this quantity. An experiment performed at Orsay by an Orsay–CERN team in an aluminum chamber led to the following empirical formula [11]:

$$\eta = 10^{\left(\frac{-2.1 \log D + 27}{6}\right)} \tag{6}$$

where $D$ is the dose in photons per meter (number of photons that hit 1 m of vacuum chamber after a certain "conditioning" time, which is the length of time the chamber is exposed to radiation).

The formula shows that the magnitude of the desorption coefficient decreases with the accumulated photon dose, since photon bombardment cleans the chamber walls.

As an example, let's calculate the time required to reach a vacuum of $10^{-9}$ Torr in a 2 GeV ring having the following characteristics:

| | |
|---|---|
| Circumference: | 200 m |
| Energy: | 2 GeV |
| Bending radius of curvature: | 5 |
| Circulating beam intensity: | 400 mA |
| Vacuum pipe diameter: | 5 cm |

The number of photons produced by the circulating beam per unit photon energy ($\epsilon$), unit time ($t$), and unit electron beam intensity ($i$) is given by

$$\frac{d^3 N_{ph}}{d\epsilon dt di} = 6.95 \times 10^{13} \frac{\rho}{E^2} \int_{\epsilon/\epsilon_c}^{\infty} K_{5/3}(x)\, dx \quad \frac{\text{photons}}{eV \cdot \text{sec} \cdot \text{mA}} \quad , \tag{7}$$

where $E$ is in GeV, $\epsilon$ and $\epsilon_c$ (critical photon energy) are in eV, and $\rho$ (bending radius) is in meters; $K_{5/3}$ is the modified Bessel function.

Integrating Eq. (7), one finds that the number of photons above the photoelectric yield ($\sim 10$ eV)

$$\frac{dN_{ph}}{dt} = 7 \times 10^{20} \text{ photons/sec} \, . \tag{8}$$

The number of molecules produced per second is

$$\frac{dN_{mol}}{dt} = \eta \frac{dN_{ph}}{dt} \, .$$

From the state equation, the throughput Q is

$$Q = \frac{PdV}{dt} = \frac{dN_{mol}}{dt}\frac{RT}{N_A} = \eta\frac{dN_{ph}}{dt}\frac{RT}{N_A} \quad , \tag{9}$$

where $N_A$ = 6.0 x $10^{23}$; $R = 8.32$ J x mole-' $K^{-1}$; $T = 300°$ K; $P$ and $V$ are the gas pressure and volume, respectively;

$$Q = 4.2 \times 10^{-21}\,\eta\frac{dN_{ph}}{dt} \quad (\text{Torr x liters/sec}) . \tag{10}$$

The conductance of a pipe of diameter $D$ as function of the distance $L$ from the pump is [12]:

$$c = \frac{1}{\frac{1}{S_p} + \frac{L}{12D^3}} \quad (\text{liters/sec}) \quad , \tag{11}$$

where $S_p$ is the pump speed in liters/sec, and $L$ and $D$ are in cm.

Let's assume there is a pump every 3 m of the storage ring, $S_p$ = 200 l/sec, and $L$ = 150 cm. The effective pumping speed (dominated by the size of the pipe) is 2000 liters/sec for the entire ring.

The value of the desorption coefficient needed to reach a vacuum of 1 nTorr is, from Eqs. (9) and (10),

$$\eta = \frac{P\,C}{4.2 \times 10^{-21}\frac{dN_{ph}}{dt}} = 7 \times 10^{-7} .$$

According to the Orsay–CERN empirical formula, this vacuum is achieved after a dose $D = 4.5 \times 10^{29}$ photons/m. From Eq. (6), we see that this dose is achieved after the chamber has been exposed to the photon flux for a time of 3.6 x 10' hours!

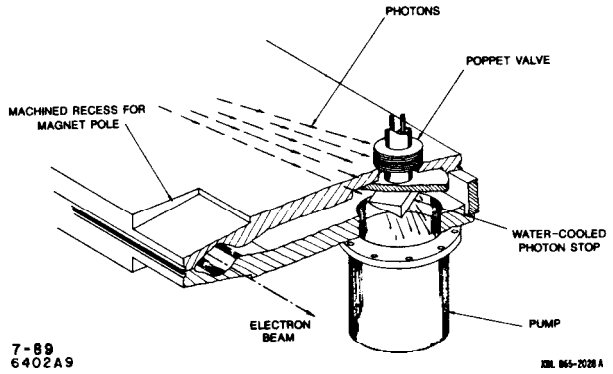


Figure 5: *Cutaway view of the Light Source vacuum chamber, showing a photon stop and titanium sublimation* pump. Figure *credit: Fig. 9.45, ALS Conceptual Design Report, LBL Report Pub-51 72.*

In order to overcome the problem of a small chamber vacuum conductance and of the gas desorbed from the chamber wall, in most designs the photon beam is made to intercept the chamber only at selected discreet locations where water cooled photon absorbers and vacuum pumps are located. This is the solution adopted, for example, by the Advanced Light Source, the Taiwan Light Source, the Advanced Photon Factory and the ESRF machine in Grenoble. Figure 5 shows a layout of the Advanced Light Source chamber with its

antichamber. The arc vacuum chamber is made of two halves of machined aluminum, welded together. The chamber geometry is such that the synchrotron radiation is intercepted by 96 photon absorbers lying outside the perimeter of the magnetic elements. The radiation emerges through a 1 cm slot that separates the chamber where the electron beam circulates from the radiation exit port. A titanium sublimation pump located underneath, and close to, the photon absorber intercepts most of the gas created by desorption. Modeling computations indicate that the designed vacuum pressure of $1 \times 10^{-9}$ Torr should be reached after an accumulated dose of 100 Ah. A very careful control of the orbit is required to prevent the photon beam from accidentally hitting the vacuum chamber at unwanted locations.

### *2.4* Intrabeam scattering (Touschek effect)

This effect was first observed in the 200 MeV storage ring ADA in 1963. It manifested itself as a fast-reduction in lifetime when the beam energy was decreased. It was interpreted by Bruno Touschek as being caused by wide-angle Coulomb collisions between electrons in the same bunch. The collision transfers transverse betatron momentum into the longitudinal and the particle is lost if the associated oscillation amplitudes are greater than the accelerator acceptance.

The Touschek effect is important at ***high-charge density,*** as in the case of short, high-current bunches with low emittance, as required by the new generation of synchrotron radiation sources. The theory of single-intrabeam scattering is well established [13] and will not be repeated here. We give a qualitative description of the basic collision mechanism and the expression for the beam lifetime.

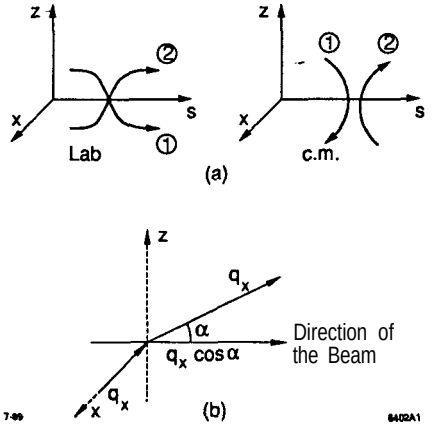


***Figure 6:*** ***(a) Collision dynamics of Touschek effect in the moving frame of the bunch. (b) The transverse momentum of the electron is transferred longitudinally at an angle a with the longitudinal direction.***

Following Ref. 13, the collision dynamics are studied in the moving frame of the bunch [Fig. 6(a)]. The relative motion occurs perpendicularly to the direction of motion and is nonrelativistic. The transverse

The transverse momentum in the center-of-mass system of the pair of particles is

$$q_x = 1/2 \cdot [(p_x)_1 - (p_x)_2] \ . \tag{13}$$

If the transverse momentum $q_x$ is transferred in the longitudinal direction at an angle $\alpha$ [Fig. 6(b)], the relativistic factor $\gamma$ magnifies the longitudinal momentum $p_s$ by

$$p_s = \gamma \ q_x \ \cos\alpha \ . \tag{14}$$

The following example, due to LeDuff, illustrates that the collision may result in a large momentum transfer in the longitudinal direction.

Consider a beam of momentum 1 GeV/c, and a particle oscillating with a maximum betatron amplitude $(x)$ of 0.1 mm. If, at the location of the collision, the value of the p-function is 10 m, then the maximum angular coordinate is $x' = x/\beta$. The relative momentum change in the longitudinal direction is

$$\frac{\Delta p_s}{|p|} = \frac{\gamma q_x}{|p|} = \frac{7''}{\beta} = 0.02 \ , \tag{15}$$

if all the transverse momentum is transferred longitudinally.

The particle is lost when the energy deviation exceeds the longitudinal acceptance of the RF system or when the amplitude of the synchrotron and betatron oscillations (the latter are excited when the longitudinal momentum transfer occurs in a nondispersive region) exceeds-the available aperture (physical or dynamical).

A study of the Coulomb cross section integrated over the particle distribution gives the half-life of the beam [13],

$$\tau_{1/2} = \frac{N_0 \ r_e^2 \ c}{87r \ \gamma^2 \ \sigma_x \ \sigma_z \ \sigma_s \left(\frac{\Delta E}{E}\right)^3_{max}} \ [D(\delta)] \ , \tag{16}$$

where $N_0$ is the number of particles per bunch; $r_e$ is the classical electron radius; $\sigma_x$, $\sigma_z$, and $\sigma_s$ are the bunch size standard deviations-horizontal, vertical, and longitudinal, respectively; and $(\Delta E/E)_{max}$ is the energy deviation acceptance of the storage ring. The function $D(\delta)$ is given by

$$D(\delta) = \sqrt{\delta} \left\{ -\frac{3}{2} e^{-\delta} + \frac{\delta}{2} \int_{\delta}^{\infty} \frac{\ln u e^{-u}}{u} \, du \right.$$
$$\left. + \frac{1}{2} (3\delta - \delta \ln \delta + 2) \int_{6}^{\infty} \frac{e^{-u}}{u} \, d \ u \right. \ . \tag{17}$$

with

$$\delta = \frac{\left(\frac{\Delta E}{E}\right)^2_{max}}{2\gamma^2 \ \sigma^2_{x'}} \ ,$$

where $\sigma_{x'}$ is the standard deviation of the angular distribution.

The expression $D(\delta)$ is a weak function of $\delta$ in the range $\delta = 0.01$-0.1.

Note that the expression only includes the beam size due in betatron space, and neglects the effect of dispersion and momentum spread on the beam size. This effect has been calculated by LeDuff [14]. Eq. (17) gives the basic parametric dependence; the scattering rate is a strong function of energy, the particle density in the bunch and the momentum acceptance of the storage ring. The Touschek effect becomes increasingly important as the energy is lowered. Figure 7 gives the Touschek half-life as a function of energy in the SRRC Light Source [10].

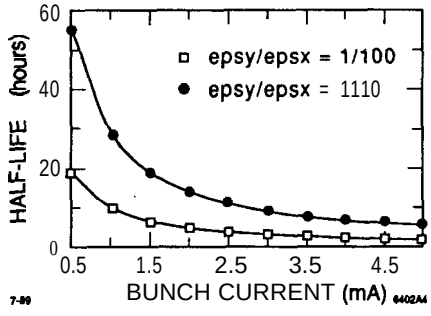


***Figure 7:*** ***Touschek lifetime*** **as a function** ***of the bunch current*** in ***the 1.3 GeV Synchrotron Radiation Source currently under construction*** in ***Taipei, Taiwan, Republic of China. The*** curves ***refer to two*** different vertical/horizontal ***emittance coupling ratios.***

The scattering process described above involve single, wide-angle scattering. Multiple small-angle Coulomb scattering occurs at high-charge density [15]. This process causes diffusion in both longitudinal and transverse phase space, resulting in increased longitudinal and transverse emittances. This phenomenon is very important for lower-energy ($\lesssim 1$ GeV) beams, but does not constitute a serious limitation in storage rings of energy 1.5-2.0 GeV and higher.

2.5 Experimental observation of gas and intrabeam scattering

In this section, we describe an experiment carried out by Gaetano Vignola [16] at the VUV ring of the Brookhaven National Laboratory. This experiment is representative of a situation in which both Touschek and gas scattering contribute significantly to a lifetime reduction. In June 1985, it was found that the beam lifetime was in gross disagreement with the theoretical predictions based on 4.0 cm of available half-aperture. The beam lifetime measurements instead predicted 2.5 cm of available aperture, and this finding was independent of the horizontal-vertical emittance coupling.

***In*** Fig. 8(a), the theoretical Touschek lifetimes are calculated for three different emittance coupling factors as a function of the horizontal aperture. The parameter $\chi$ is the ratio of vertical to horizontal emittances.

The experimentally measured lifetime is the sum of the gas scattering and Touschek contributions:

$$\frac{1}{\tau_{exp}} = \frac{1}{\tau_{gas}} + \frac{1}{\tau_{Touschek}} \quad . \tag{18}$$

Fig. 8(b) depicts the curve of gas scattering as a function of aperture, as calculated from Eq. (18)

and Fig. 8(a) for three different coupling factors. Since the gas scattering lifetime does not depend on the coupling, the three curves must intersect at an aperture corresponding to the real aperture limit: 2.5 cm. This result is in excellent agreement with the known available aperture of 2.7 cm (limited by a septum magnet).

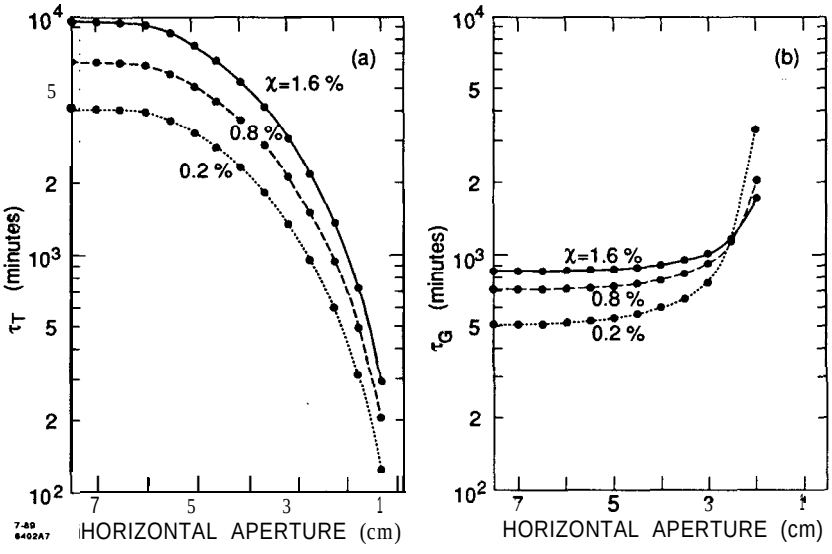


Figure 8: *(a) Touschek* lifetime in *the 750 Me V Light Source at Brookhaven National Laboratory calculated* for *three different values of the emittance coupling factor* $\chi$. *Electron energy: 750 Me V; current* per *bunch:* 3.9 $mA$. *(b)* Gas-scattering lifetime *as a function of machine aperture.*

## 3. NONACCEPTANCERELATED EFFECTS

In this section, we discuss three effects that are not directly related to the betatron or momentum acceptance of the storage ring: coupled bunch oscillations, single bunch oscillations, and ion trapping.

### 3.1 Coupled bunch oscillations

In order to achieve high-photon brilliance, accelerator designers strive to design machines that can store a large beam current. Because of the limit on the number of electrons that can be packed in single bunch, the design- tries to accommodate as many circulating bunches as possible. The electromagnetic field of "long memory" resonant objects in the ring tends to couple the motion of the bunches. Under certain conditions that depend on the characteristics of the coupling impedance of the resonant objects, a positive feedback develops by which the voltage induced by the beam interacts with the beam itself, leading to an instability.

The instability can be longitudinal, resulting in growth of synchrotron oscillation amplitudes, or transverse (growth of betatron amplitudes). The theory has been developed by several authors [17]. Considering first the longitudinal motion, the fastest-growing instability is normally the one wherein each bunch behaves as a single rigid particle (dipole mode). The growth time $\tau$ is given by:

$$\tau = \frac{e\, I_{av}\, \eta\, \omega_0^2}{4\pi\ E\ \omega_{s0}} \sum_{P=0}^{\infty} \left[ (P\,M - l)\ \ R - - (P\,M + l)\ \ R^{+} \right], \tag{19}$$

where $I_{av}$ is the average circulating beam current, $\eta$ is the momentum compaction function, $\omega_0$ is the angular revolution frequency, $E$ is the electron energy, and $\omega_{s0}$ is the small-amplitude synchrotron frequency.

The summation extends over all the frequencies that can resonate with the cavity-like objects in the ring. $R^+$ and $R^-$ denote the resistive part of the impedance at the frequencies $(PM + l)\omega_0 + \omega_{s0}$ and $(PM - l)\omega_0 - \omega_{s0}$. $M$ is the total number of bunches, and $l$ is the mode number. To define the latter, we note that, given $M$ bunches of equal charge, equally spaced, closure and symmetry require that the phase of oscillation of each bunch relative to the preceeding one be the same for all bunches. The phase shift from bunch to bunch is given by $2\pi\, l/m$. The modes of oscillation of a four-bunch system are shown in Fig. 9.

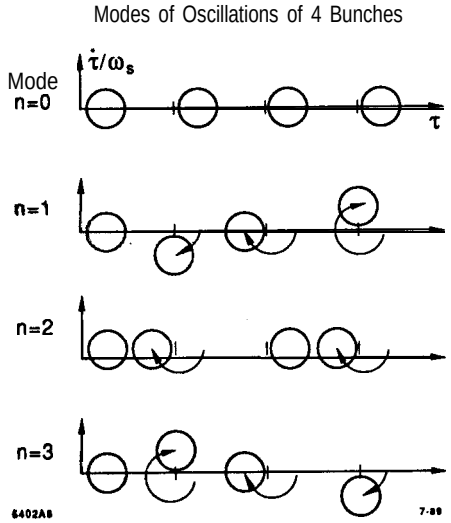


***Figure 9:*** ***Modes of*** oscillation ***of four bunches.***

As we mentioned earlier, resonant objects distributed around the ring contribute to the impedances $R^+$ and $R^-$. These objects are given by discontinuities that cause a sudden change in vacuum chamber cross section. Since the condition of long memory of the wakefields requires a high Q resonator, the RF cavities are, normally, the main offending objects.

Beside the rigid bunch mode, higher-order modes can develop (quadrupole, sextupole, etc.), wherein the shape of the bunches is modulated.

The instability develops when its growth time is shorter than the longitudinal radiation damping time. The experimental observations indicate that the longitudinal coupled bunch oscillations rarely cause beam loss: the momentum oscillation increases its amplitude until the nonlinearity of the RF bucket introduces enough decoherence to damp the instability. This instability does, however, represent a potentially serious performance degradation. Its effects are: increase in bunch length, increase in spot size from bending magnet radiation (via the increased momentum spread), fluctuating intensity of the light, low accumulation rate, and short lifetime.

It is interesting to note, in Eq. (19), the dependence of the growth time of the instability on the momentum compaction function $\eta$. As the focusing of the lattice increases to achieve smaller spot size, the momentum compaction function normally decreases also, and makes it more difficult to achieve stable operation.

Resonant conditions can be derived from ***transverse coupled bunch oscillations*** [18]. These oscillations are driven by transverse deflecting electromagnetic fields that decay slowly and act on the following bunches. The transverse instability usually has longer growth times than the longitudinal one.

Several measures can be taken to increase the growth time for the instabilities. The most effective one is to limit the impedance of the ring by careful design of the vacuum chamber, the accelerating cavities and other discontibuities. Special care is taken in damping the nonaccelerating modes of the RF cavities by the introduction of antennas. In case of a chain of cavities, introducing a slight shift in the resonant frequencies of the nonaccelerating modes may help, since these modes do not all overlap at the same frequencies. Splitting the synchronous frequencies of the individual bunches with a low harmonic cavity can also be effective in decoupling the bunches.

For the transverse oscillations, RF quadrupoles that split the betatron frequencies of the bunches and decouple the transverse motion may prevent the onset of the instability.

Landau damping, or the introduction of nonlinearities to the motion, can theoretically be obtained in the longitudinal case via the addition of a higher harmonic cavity (for instance, the fourth harmonic of the main accelerating frequency). In the transverse plane, Landau damping usually requires octupoles to introduce amplitude-dependent tune shifts. For high-brilliance sources, however, the small longitudinal and transverse emittances require very strong nonlinearities for Landau damping that can be detrimental to the lifetime of the beam. This is particularly true for the transverse instabilities, where octupoles tend to reduce the dynamic aperture.

The most effective way to damp coupled bunch oscillations is to use the feedback system. In the longitudinal plane, a beam monitor detects a change in position in the horizontal axis dae to a change in energy, or a change in the arrival time at a fixed location. The signal is fed to a special RF cavity that acts on the beam in such a manner as to damp the growth of the oscillations. For the longitudinal instability, the maximum voltage per turn $V$ required by the feedback cavity is

$$V = \frac{2E}{\tau f_{rev}} \frac{\Delta E}{E} , \tag{20}$$

where $\Delta E/E$ is the relative energy error acted on by the feedback system, $f_{rev}$ is the revolution frequency, and $\tau$ is the rise time of the instability.

For transverse oscillations, the betatron amplitude is detected and fed back to a transversely deflecting device.

The technological limit of the feedback system is represented by the fact that, in order to act on each individual bunch, the frequency band of the system must be large, of the order of half of the bunch repetition frequency. This, coupled with the voltage normally required for fast damping [Eq. (20)], poses a limit (practical, if not conceptual) to the total number of bunches that can be stored in the ring.

### 3.2 Single-bunch instabilities

These instabilities are driven by short wavelengths (of the order of the bunch length) and short memory wakefields in cavity-like objects in the ring. The ***longitudinal microwave*** instability [19], also known as

turbulent bunch lengthening, causes the momentum spread to blow up and increases the length of the bunch.

The maximum peak current that can be stored in a single bunch before bunch lengthening occurs is given by

$$\hat{I} = \frac{2\pi \eta (E/e)}{|Z/n|} \left(\frac{\Delta P}{P}\right)^2 , \qquad (21)$$

where $\Delta P/P$ is the rms momentum spread in the beam, $E$ is its energy, e is the electron charge, and $\eta$ is the momentum compaction function. $|Z/n|$ is the modulus of the effective longitudinal impedance in the high-frequency region divided by the harmonic $n$ of the revolution frequency. $|Z/n|$ is a very important quantity that depends on the total impedance of cavity-like objects distributed around the ring. Typical contributors to this "broadband impedance" are the accelerating cavities, beam position monitors, bellows, vacuum chamber discontinuties in the transition from a regular cross section to the smaller cross section of an undulator, etc.

In older-generation machines, $|Z/n|$ is of the order of tens of ohms. In the radiation sources presently under construction, designers try to keep the value below 1 ohm.

The longitudinal microwave instability rarely causes beam loss, but it does increase the momentum spread and the bunch length. This may be a problem for those users who require very short photon pulses, as might be the case for time-resolved experiments.

The ***transverse microwave instability*** [20] is also called "fast blow-up instability." This instability leads to beam loss. Fortunately, its current threshold is usually higher than that of the longitudinal instability.

### 3.3 Ion trapping

The phenomenon of ion trapping by the potential well of the circulating electron beam has been observed in all electron synchrotron radiation sources. This phenomenon can manifest itself as transverse beam blow-up, but most commonly as sudden loss of beam lifetime. This is an elusive and poorly understood process, usually blamed for any unexplainable beam quality deterioration!

Using positrons instead of electrons gets rid of the problem. This represents a sensible solution for higher-energy radiation sources (6-8 GeV), where the cost of a positron facility represents a relatively small portion of the total cost of the machine. In lower-energy radiation sources the cost impact is greater; for this reason, they are generally designed for electrons. The option usually is left open to accelerate positrons later on, should ion trapping be a serious performance limitation.

Ion trapping is caused by the ionization of the residual gas by the electron beam. Ions are produced at thermal velocities, and almost at rest in the laboratory frame (a few hundred m/sec) compared to the electron velocity. The ions receive transverse kicks at successive passages of the $e^-$ bunches, which act as a focusing force. The outcome of the cumulative effect of all the kicks is one of the following:

- ions remain in the potential well of the electrons (ion trapping); or
- ions escape the potential well (no ion trapping).

The effects of trapped ions on the electron beam are:

- increased gas pressure, multiple gas scattering with associated reduced lifetime.
- space charge effects that cause tune shift and tune spread and, ultimately, particle loss.
- coherent electron ion-oscillations are also possible.

The stability of the ion motion under the conditions described above have been studied by several authors [21]. The starting point of all the models is to study the motion in the linear approximation. The ions feel a periodic focusing kick (the electron beam) followed by a drift (time between transits of electron bunches). The transformation matrix for a period (bunch crossing + drift) is, at the start of accumulation,

$$\begin{pmatrix} y \\ \dot{y} \end{pmatrix} = \begin{pmatrix} 1 & t_b \\ 0 & 1 \end{pmatrix} \begin{pmatrix} 1 & 0 \\ -a & 1 \end{pmatrix} \begin{pmatrix} y_0 \\ \dot{y}_0 \end{pmatrix} , \tag{22}$$

for ion oscillations in the vertical plane, and where

$$a = \frac{N}{n} \frac{2 r_e c}{\sigma_y (a, + \sigma_y)} \frac{1}{A} ,$$

$A$ is the atomic number of the ion, N is the total number of particles per beam, $n$ is the number of bunches, $\sigma_x$ and $\sigma_y$ are the transverse electron beam sizes (standard deviations), $t_b$ is the interbunch time separation, $r_e$ is the classical electron radius, and c is the speed of light.

According to the standard stability criterion, the motion is stable (ions are trapped) if

$$-2 < Tr(M) = \quad 2 - a \times t_b < 2 \quad .$$

This corresponds to a ***critical*** ion mass

$$A , = \frac{r_e N C}{2n^2 \sigma_y (\sigma_x + \sigma_y)} , \tag{23}$$

where $C$ is the ring circumference.

All the ion species for which $A > A,$ accumulate.

As the ions accumulate, the defocusing force of the ion cloud must be taken into account; the drift space is now replaced by a defocusing lens and the ion stability changes:

$$A > A , - k d_i$$

where

$$k = \pi r_e \left(\frac{C}{n}\right)^2 \frac{1}{1 + \sigma_y/\sigma_x}$$

and $d_i$ is the ion density.

As the ions accumulate, lighter and lighter ions are trapped. This process is called the ion ***ladder.***

Ions can be made unstable by leaving one or more gaps in the train of bunches, in analogy with exciting the half-integer resonance in the ion motion. This is a very effective method to suppress ions, successfully applied in several synchrotron radiation sources. The length of the gap that is required varies for different machines, but is, typically, of the order of one-third of the ring circumference.

Clearing electrodes are also effective in suppressing the ions. A difference of potential of a few kV over 2-3 cm across the vacuum chamber can be effective in taking the ions out of the potential well of the electrons. This field has no effect on the highly energetic circulating electrons. For larger currents and smaller gaps, stronger clearing fields are required that might be difficult to implement. Ion clearing becomes more effective if the clearing field is modulated at the oscillating frequency of the ions. However, when the ion reaches the nonlinear region of the electron charge density, its oscillating frequency changes and an oscillating field tuned to the linear frequency becomes less effective. In this case, a combination of static and oscillatory field is more effective [22]:

- the static field drags the ion in the nonlinear part of the field.
- the oscillating field, tuned at the ion shifted frequency, increases its amplitude out of the electron beam and the ion is lost.

## 4. POSITIONAL STABILITY OF THE PHOTON BEAM

Movement of the ground or local temperature changes causes the magnet support structure to move. As a consequence, the magnets also move, and so do the electron beam and the emitted photon beam. In the new generation of light sources, the problem is exacerbated by the fact that these machines are characterized by small electron beam size, thus

- small photon spot size and consequent tight orbit stability tolerance (a fraction of the spot size).
- increased sensitivity to quadrupole movement because of stronger electron optics focusing.

Thus, it appears that the severity of the photon beam stability problem scales like the square of the photon brilliance.

In this section, we discuss the stability requirements, the causes of photon beam movement and possible prevention and cures.

### 4.1 Stability requirements

The major effects of the photon beam movement depend on the detail of the beamline, but basically are the following:

| | |
|---|---|
| Position change: | loss of photon flux. |
| Angle change: | loss of photon flux and wavelength shift. |

As an example, consider the positional stability of a beamline with entrance slit. Let's assume that the slit is open at $\pm 2$ standard deviation of the photon beam size (assumed of Gaussian shape). A simple calculation shows that, for a 1% throughput stability, the photon beam must be stable within 17% of the standard deviation of its transverse size. For a machine like the Advanced Light Source, this requirement implies an orbit stability of the electron beam of 33 $\mu$m horizontally and 6 $\mu$m vertically. The relationship

between the quadrupole positional stability and the orbit movement is given by

$$\langle \Delta x,y \rangle_{orbit} = \frac{\sqrt{\beta_{x,y}(s)}}{\sin(\pi \nu_{x,y})} \left[ \sum_i K_i^2 l_i^2 \beta_{x,y,i} \right]^{1/2} \langle \Delta x,y \rangle_{quad} \quad , \tag{24}$$

where < Ax, y $>_{orbit}$ is the rms probability of horizontal and vertical orbit shifts, $\beta_{x,y}(s)$ is the p-function at the orbit observation point, $\nu_{x,y}$ are the betatron tunes, $K_i l_i$ is the integrated strength of the i-th quadrupole, $\beta_{x,y,i}$ is the p-function value at the i-th quadrupole location, and < Ax, y $>_{quad}$ is the rms value of the horizontal and vertical quadrupole movements.

Eq. (24) gives the dependence of the orbit sensitivity to quadrupole misalignments on the strength of the quadrupoles. For the example of 1% throughput stability given above, Eq. (24) gives an rms quadrupole positional stability of the order of 1 $\mu$m!

4.2 Causes of magnet movement

(a) Ground movement (seismic motion; ground settlement, traffic, cranes, heavy machinery, etc.).

*(b)* Temperature effects (temperature changes and gradient in magnet support structure, thermal distortions in mirrors and monochromators).

(c) Electrical disturbances (power supply ripple, booster synchrotron cycling, long-term drift of magnetic field).

*(d)* Magnetic effects on orbit (hystereses after orbit changes, ramping, magnet cycling). Changes of insertion device field strength.

(e) Electron beam instabilities (coupled bunch oscillation-ion trapping).

The parameters influencing the sensitivity of the orbit to mechanical and thermal perturbations are the amplitude and wavelength of the perturbation. The longest wavelength of interest is given by the length of the ring diameter + beamlines. Assuming a velocity of ground motion of 1.5 km/sec and a facility diameter of 100 m gives frequencies of interest of about 15 Hz and higher. Frequencies corresponding to a betatron wavelength are particularly sensitive (about 50-100 Hz).

The conditions vary from site to site, but, for most machines, in the frequency domain above 1 Hz, most of the important disturbances are manmade, with typical oscillation amplitudes of 0.1-1.0 $\mu$m. Thermal effects are probably the most important cause of beam movement.

4.3 Prevention and cures

Several measures are being taken to reduce this problem. To reduce the magnetic effect (magnetic field ramping), most third-generation machines inject at the operating energy of the storage ring. Care is taken in the design of the magnet support structure: the mechanical resonant frequencies are damped where necessary, and effort is made to reduce the temperature gradient in the magnet support. The environmental sources of noise should be minimized: the geographical location is conveniently chosen and one tries to decouple the ring from the source of vibration (by introducing damping in support and floor construction). Air conditioning (local or global) may be required. After all of the above is done, however, it is unlikely that the quadrupoles will not move by more than the estimated tolerance ($\mu$m). For this reason, nearly all modern synchrotron radiation sources use feedback systems to stabilize the orbit.

Various methods of feedback systems can be used to:

- Measure the orbit movement and correct the electron orbit.
- Measure the photon beam movement and correct the electron orbit.
- Measure the photon beam movement and correct the photon beam trajectory (with mirrors).

Orbit feedbacks may consist of a localorbit bump in the insertion device region, or they may compensate globally for the main closed orbit harmonics (those close to the value of the betatron tunes). The practical limitations of the feedback systems are represented by the beam position monitor sensitivity (about 10 microns for a state of the art device) and by the frequency response of the system. The latter is limited, usually, by the magnetic field attenuation in the vacuum chamber to, typically, 50-100 Hz.

Acknowledgments

The author wishes to thank Kurt Kennedy for his valuable contribution to some vacuum aspects discussed in this paper, and is also grateful to Gaetano Vignola for his information on the aperture experiment carried out at the UV light source at Brookhaven National Laboratory.

References

[I] A. Ropert, these proceedings.

[2] l-2 GeV synchrotron radiation source, Conceptual Design Report, Lawrence Berkeley Laboratory Report PUB-5172 Rev.

[3] M. Sands, SLAC Report 121 (1970).

[4] See, for instance, G. Guignard, Nonlinear dynamics, and A. Chao, Comments on nonlinear dynamics studies in storage rings, AIP Conf. Proc. 184, Physics of Particle Accelerators. See also Nonlinear dynamics aspects of particle accelerators, Proc., Sardinia, 1985, Lecture Notes in Physics, 247, Springer-Verlag. Proc. 2nd Advanced Beam Dynamics Workshop, Lugano, Switzerland, April 11-16, 1984, CERN Report 88-04.

[5] M. Sands, SLAC Report, SLAC-TN-69/8 and 69/10 (1969). C. Pellegrini, Nuovo Cimento 64A (1969) 447.

[6] A. Ropert, The ESRF lattice and its sextupole correction scheme, Proc. Jaeri-Riken Symposium on Accelerator Technology for the High-Brilliance Synchrotron Radiation Sources, Tokyo, Japan, September 5-6, 1988. E. A. Crosbie, Improvement of the dynamic aperture in Chasman-Green lattice design light source storage rings, Proc. 1987 IEEE Particle Accelerator Conf., Washington, D.C., March 16-19, 1987. P. Certain, Super ACO Report 88-19, Rubrique: Optique, April 1988.

[7] B. V. Chirikov, Report 267 of the Nuclear Physics Institute of the Siberian Section of the USSR Academy of Sciences, Novosibirsk, 1969 (CERN Trans. 71-40).

[8] Fig. 2 summarizes the information collected by the author from various sources. The author believes the information to be correct, but apologizes for any inaccuracy that might be present.

[9] J. Haissinski, Thése Laboratoire de l'Accelerateur Lineaire, Orsay (1965). C. Bernardini *et al.,* Lifetime and beamsize in electron storage rings, Proc. Int. Conf. on High Energy Accelerators, Dubna, 1963, p. 411415.

[10] Design Handbook of the Synchrotron Radiation Research Center (Taipei, Taiwan, Republic of China, April 1989), p. 1.17-3.

[11] 0. Grobner *et al.,* Vacuum 33 (1983) 7. The empirical formula (6) was derived by fitting the experimental points by K. Kennedy.

[12] A. Roth, Vacuum technology (North-Holland, 1976).

[13] H. Bruck, Circular particle accelerators, translated as Los Alamos Scientific Laboratory Report LA-TR-72-10 Rev.

[14] J. LeDuff, Single and multiple Touschek effect, Proc. Int. Workshop on Synchrotron Radiation Instrumentation, Taipei, Taiwan, Republic of China, February 22-27, 1988.

[15] J. Bjorken and S. K. Mtingwa, Particle Accelerators, 13 (1983) 115.

[16] G. Vignola, private communication.

[17] J. L. Laclare, Bunched beam instabilities, Proc. 11th Int. Conf. High-Energy Accelerators, CERN, Geneva, 1980, (Birkhauser, Basel) pp. 526-539. J. M. Wang, Brookhaven National Laboratory Report BNL-51302 (December 1980). C. Pellegrini and M. Sands, Stanford Linear Accelerator Report PEP-258 (October 1977).

[18] J. L. Laclare, Bunched beam instabilities, Proc. 11th Int. Conf. High-Energy Accelerators, CERN, Geneva, 1980, (Birkhauser, Basel) pp. 526-539. B. Zotter and F. Sacherer, Transverse instabilities of relativistic particle beams in accelerators and storage rings, Theoretical aspects of the behavior of beams in accelerators and storage rings, 13, p. 175.

[19] A. Hoffmann, Single-beam collective phenomena-longitudinal, Theoretical aspects of the behavior of beams in accelerators and storage rings, 13, p. 139.

[20] R. D. Ruth and J. N. Wang, IEEE Trans. Nucl. Sci. NS-28 (1981) 2405.

[21] Y. Baconnier and G. Brianti, CERN/SPS/80-2 (1980). Y. Baconnier, Neutralization of accelerator beams by ionization of the residual gas, General Accelerator Physics, Proc. CERN Accelerator School, Gif-sur-Yvette, Paris, France, September 3-14, 1984, CERN 85-19, p. 267.

[22] C. J. Bocchetta and A. Wrulich, Sincrotrone Trieste Report ST/M-88/26.